The Analysis of Three-dimensional Oxidation Process with Elasto-viscoplastic Model

Jun-Ha Lee[a] and Hoong-Joo Lee
Department of Computer System Engineering, Sangmyung University, Anseo-dong, Chonan-si, Chungnam 330-720, Korea

[a]E-mail : junha@smu.ac.kr

(Received July 15 2004, Accepted September 9 2004)

This paper presents a three-dimensional numerical simulation for thermal oxidation process. A new elasto-viscoplastic model for robust numerical oxidation simulation is proposed. The three-dimensional effects of oxidation process such as mask lifting effect and corner effects are analyzed. In nano-scale process, the oxidant diffusion is punched through to the other side of the mask. The mask is lifted so the thickness of oxide region is greatly enhanced. The compressive pressure during the oxidation is largest in the mask corner of the island structure. This is because the masked area near the corner is surrounded by an area larger than the others in the island structure. This stress induces the retardation of the oxide growth, especially at the masked corner in the island structure.

Keywords : Oxidation, Three-dimension, Elasto-viscoplastic, Lifting effect, Corner effect

1. INTRODUCTION

The characteristics of nano-scale transistors in GSI technologies are strongly affected by multi-dimensional device structure. Process simulations have contributed to a better understanding of device physics and to the development of new processing techniques. Therefore, process simulation has established itself as an important tool for process and device development of this age. Isolation technique has a very important role in nano-scale process. The trench isolation process has been widely used for device isolation due to its area merit and good isolation characteristics[1]. Despite the impressive advantage of shallow trench isolation, a variety of new difficulties associated with the new launched STI structures arise. The regions of the channel near the edges of the device will behave much differently than the region at the center of the mesa. The three-dimensional modeling verify that the corner regions have a lower electrical behavior than do the center regions[2]. With device sizes shrinking, three-dimensional oxidation process simulations are required to predict the accurate shape of the oxide, the stress distribution and the three-dimensional effects, such as corner effect and mask lifting effect at the top edge of trench structure. But, it is very difficult for two-dimensional simulations to predict the three-dimensional effects or understand the 3-D behavior[3]. Therefore accurate simulations of these three-dimensional effects are needed in order to ensure optimal control of the technological oxidation process. To achieve the shallow junction of source/drain and prevent the deactivation of dopant, the lower process temperature is required. In addition, for small three-dimensional geometry and more accurate stress distribution, a new robust model is needed.

In this paper, we developed the three-dimensional process simulator of oxidation with elasto-viscoplastic model. In this model, the oxidant diffusion is solved by BEM(Boundary Element Method) in three dimensions. The stress factor is incorporated into oxidant diffusivity and reaction rate. The nitride mask is treated as elastic beam, which is bent when the window region is large enough to compare the thickness of the final oxide thickness, but when small geometry is used, it is just lifted rather than bent.

2. PHYSICAL MODEL OXIDATION

Numerical oxidation mechanisms can be divided by three steps[4]: oxidant diffusion, chemical reaction and oxide flow or deformation. Step one, the oxidant diffuses from the ambient through the oxide to the oxide and silicon interface. Once it reaches the silicon surface, step two, the oxidant reacts with silicon atom to form SiO_2. At this point, a volume of silicon expands to 2.25

volumes of oxide. This volume expansion causes a flow of oxide with shape deformation of the existing oxide. The procedure for overall three-dimensional oxidation calculation is given in the flow-chart of Fig. 1.

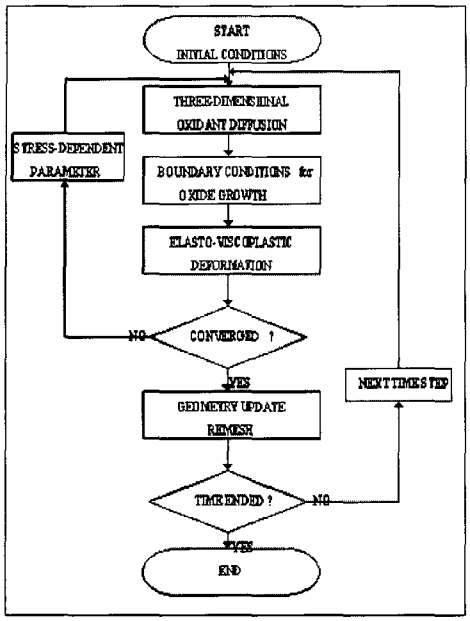

Fig. 1. Oxidation simulation flow chart.

2.1 Oxidant diffusion

The first step of oxidation is based on a steady-state oxidant diffusion. The oxide layer is formed at the Si-SiO_2 interface as a result of the chemical reaction between silicon and oxidants(OH- ions or O_2 molecules). The oxidants reach the interface after diffusing through the growing oxide. Oxidant diffusion can be modeled by a three-dimensional diffusion equation as follows:

$$D_{eff}\nabla^2 C = 0 \tag{1}$$

Where C and D_{eff} are the concentration of oxidant and the stress-dependent oxidant diffusivity, respectively. Boundary conditions for (1) used the oxidant flux conditions of the Deal-Grove's one-dimensional model [5] in a three-dimensional extension. It is given by

$$F \cdot n = 0 \tag{2}$$

where F and n are oxidant flux and normal unit vector, respectively. The first step in the algorithm is to solve the three-dimensional oxidant diffusion equation based on the BEM[6] which has the advantage of stability, rapid computer execution and moving boundary problem. A formulation of the steady-state oxidant diffusion equation using the Green's function method results in a boundary integral representation. This integral equation is discretized after volume integration and finally the linear equation set is obtained which is solved using a direct linear solver.

2.2 Stress dependent parameters

For an accurate estimation of the oxide shape, the stress effect on the oxide growth is considered by using two stress dependent physical parameters[7,8]. They are the surface reaction rate k_s, and the oxidant diffusivity D_{eff} as proposed by Kao et al.[9].

$$k_s = k_0 \exp(\frac{\sigma_{nn} V_k}{kT}) \tag{3}$$

$$D_{eff} = D_{eff} \exp(-\frac{PV_D}{kT}) \tag{4}$$

Here, σ_{nn} , P , V_k , and V_D are the normal stress(negative sign for compression) on the silicon/ oxide interface, the pressure in oxide(positive sign for compression), the reaction jump volume in silicon to oxide and the active diffusion volume, respectively. The zero stress parameters, K_0 and D_0 are derived from the experimental linear-parabolic rate constants. The nitride mask bending stress P_m on the nitride and oxide interface is calculated in three-dimensions by the beam bending theory as

$$P_m = E_{mask} I(\frac{\partial^4 T}{\partial x^4} + 2\frac{\partial^4 T}{\partial x^2 \partial y^2} + \frac{\partial^4 T}{\partial y^4}) \tag{5}$$

where E_{mask} , I , and T are the Young's modulus of nitride, the moment of inertia and the position of oxide surface, respectively.

2.3 Elasto-viscoplastic model

The theory of elasto-viscoplastic model[10,11] is described in this subsection. For a nonlinear continuum problem, it is assumed that the total strain, ε , can be separated into elastic, ε_e , and viscoplastic, ε_{vp} , components. That is so the total strain rate can be expressed as

$$\varepsilon' = \varepsilon'_e + \varepsilon'_{vp} \tag{6}$$

where (`) represents differentiation with respect to time. The total stress rate depends on the elastic strain rate according to

$$\sigma = D\varepsilon'_e \tag{7}$$

where D is the elasticity matrix. The onset of viscoplastic behavior is governed by a scalar yield condition of the form

$$F(\sigma,\varepsilon_{vp})-F_0=0 \tag{8}$$

in which F_0 is the uniaxial yield stress which may itself be a function of a hardening parameter. For frictional materials F_0 is the equivalent yield stress and assumed that viscoplastic flow occurs for values of $F > F_0$ only.

Viscoplastic strain rate depends only on the current stress, so that

$$\varepsilon'_{vp}=f(\sigma) \tag{9}$$

The relationship can be generalized to include strain hardening, temperature dependence and the influence of the state of dependent variables, such as damage parameters for rupture theories, which can also be considered.

In case of F = Q, equation (9) reduces to

$$\varepsilon'_{vp}=\gamma<\Phi(F)>\frac{\partial F}{\partial\sigma}=\gamma<\Phi>a \tag{10}$$

where, γ is a fluidity parameter controlling the plastic flow rate and a is the flow vector.

3. SIMULATION RESULTS

Two typical mask structures, which are hole and island structures, are used in the simulations to study three-dimensional effects on oxide growth. Figure 2(a)-(b) shows the hole structure simulation results. Figure 2(a) shows schematically the initial hole or contact structure. A square nitride mask is defined in the hole structure in which the width of the nitride is same as the length. Figure 2(b) shows the 1/4 cutting part of hole structure because of the easy to understand the three-dimensional oxide shape. The process condition is: 400 Å Nitride, 50 Å pad-oxide, 5900 Å thickness of grown oxide. And simulated structure size is 2 μm by 2 μm. The patterned nitride mask sizes were from square of 1.0 μm × 1.0 μm to square of 0.05 μm × 0.05 μm. The relationship between the center-point thickness in pad-oxide region and nitride width is shown in Fig. 3. The mask lifting effect or strong three-dimensional narrow mask size effect is explained by the large encroachment of the oxide due to oxidant diffusion punchthrough. In the case of small mask size structure, nitride stress is no longer sufficient to suppress the upward growing oxide force.

Figure 4(a)-(c) shows the calculated three-dimensional oxide shapes for island structure. Figure 4(a) shows schematically the initial island structure before oxidation. In simulation, the island structure size is 1.0 by 1.0 μm squares and the window region is 0.2 by 0.2 μm squares. The thickness of grown oxide region is 5000 Å. This oxide thinning effect is due to the reduction of the oxidant diffusion. Oxidant diffusion is restricted by the small window area.

Figure 4(b) shows the three-dimensional view of the final oxide shape without mask. The oxide growth behavior under the corner of the mask edge strongly depends on the initial mask structure. In Fig. 4(c), which shows the contour line with top surface of oxide, at corner

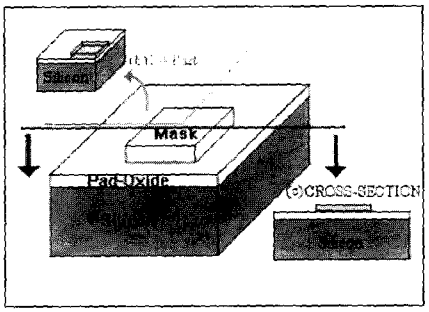

(a)

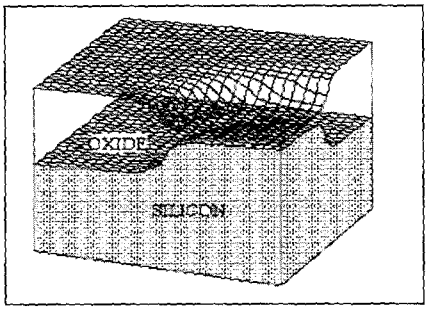

(b)

Fig. 2. Mask lifting effect and oxide punchthrough.
(a) Simulated structure with an indication cut line.
(b) 1/4 part plot of Hole structure simulation.

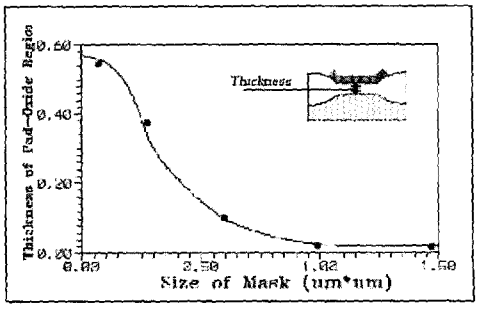

Fig. 3. Relationship of bird's beak thickness versus nitride width.

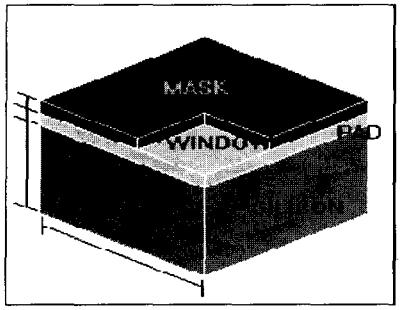

(a)

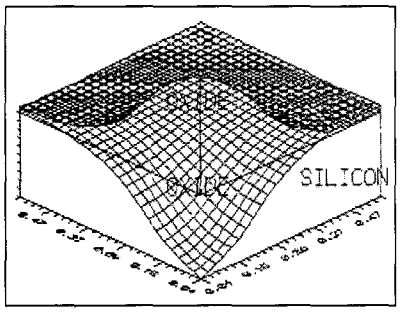

(b)

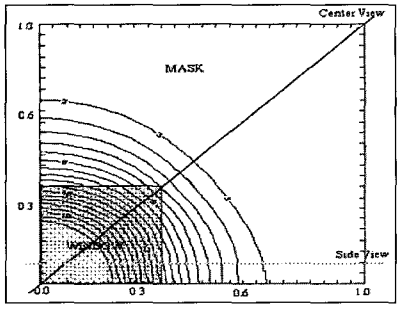

(c)

Fig. 4. Three-dimensional simulation in island struc-ture: (a) simulated island structure, (b) three-dimensional view, and (c) contours of oxide surface.

of the mask edge, the rounding of the oxide is simulated well. At the corner, larger compressive pressure is caused by the nitride mask bending in the island structure. The compressive pressure during the oxidation is largest in the mask corner of the island structure. This is because the masked area near the corner is surrounded by an area larger than the others in the island structure[12]. This stress induces the retar-dation of the oxide growth, especially at the masked corner in the island structure. During initial oxidation, the compressive pressure is increased by the nitride mask bending. After that, it is gradually decreased with decreation of the oxide growth rate. This is the reasons of the bird's beak punchthrough effect.

4. CONCLUSION

For accurate calculations of oxide growth and stress distributions in three dimensions, a new numerical model and procedure has been proposed. Also, in small geometry there must be consideration of the three-dimensional effects of oxidation. Using the proposed elasto-viscoplastic model with the stress parameters, we developed the three-dimensional thermal oxidation numerical simulator. A simulation based on the model was carried out for three-dimensional hole and island structures. It can provide useful information about three-dimensional oxidation effects such as corner rounding and mask lifting effects, stress distribution, and oxide shape.

REFERENCES

[1] S. Wolf and R. N. Tauber, "Silicon Processing for the VLSI Era-volume 1", Lattice Press, p. 265, 2000.
[2] R. B. Marcus and T. T. Sheng, "The oxidation of shaped silicon surfaces", Extended Abstracts, Electrochem. Soc. Mtg., Vol. 129, p. 1728, 1982.
[3] S. Wolf, "Silicon Processing for the VLSI Era-volume 4", Lattice Press, p. 433, 2002.
[4] H. Umimoto and S. Odanaka, "Three-dimensional numerical simulation of local oxidation of silicon", IEEE Trans. on Electron Devices, Vol. 38, No. 3, p. 505, 1991.
[5] C. S. Rafferty, L. Borucki, and R. W. Dutton, "Plastic flow during thermal oxidation of silicon", Appl. Phys. Lett., Vol. 54, No. 16, p. 1516, 1989.
[6] D. B. Kao, J. P. McVittie, W. D. Nix, and K. C. Saraswat, "Two-dimensional thermal oxidation of silicon-II. modeling stress effects in wet oxides", IEEE Trans. on Electron Devices, Vol. 35, No. 1, p. 25, 1988.
[7] B. E. Deal and M. Sklar, "General relationship for the thermal oxidation silicon", J. Appl. Phys., Vol. 36, No. 12, p. 3770, 1965.
[8] Wang Jimin, Li Yu, and Li Ruiwei, "An improved silicon-oxidation-kinetics and accurate analytic model of oxidation", Solid-state Electronics, Vol. 47, Iss. 10, p. 1699, 2003.
[9] C. A. Brebbia and J. Dominguez, "Boundary Elements: An Introductory Course, 2nd ed.", Computational Mechanics Publications, p. 132, 1992.
[10] C. Collard, I. Roch, L. Buchaillot, and X. Wallart, "A robust numerical procedure for stress dependent 2d-oxidation simulation", NUPAD IV, p. 21, 1992.
[11] S. M. Suh, M. R. Zachariah, and S. L. Girshick, "Numerical modeling of silicon oxide particle formation and transport in a one-dimensional low-pressure chemical vapor deposition reactor", Journal of Aerosol Science, Vol. 33, Iss. 6, p. 943, 2002.
[12] T. Furukawa and J. Mandelman, "Process and device simulation of trench isolation corner parasitic device", Electrochem. Soc. Mtg. Abs., p. 329, 1988.